

A modular perspective to the jet suppression from a small to large radius in very high transverse momentum jets

Om Shahi,¹ Vaishnavi Desai,² and Prabhakar Palni^{2,*}

¹*Department of Physics, BITS Pilani, Goa.*

²*School of Physical & Applied Sciences, Goa University, Goa.*

In this work, we extend the scope of the JETSCAPE Framework to cover the jet radius(R) dependence of the jet Nuclear Modification factor (R_{AA}) for broader area jet cones, going all the way up to $R = 1.0$. Our primary focus has been the in-depth analysis of the high- p_T inclusive jets and the quenching effects observed in the Quark-gluon plasma formed in the Pb-Pb collisions at $\sqrt{s_{NN}} = 5.02$ TeV for the most-central (0-10%) collisions. Nuclear modification factor (R_{AA}) is calculated for inclusive jets to compare with the experimental results collected at the ATLAS and the CMS detectors in the jet- p_T range from 100 GeV up to 1 TeV. The results predicted by the JETSCAPE are consistent in the high p_T range as well as for extreme jet cone sizes. We also calculate the double ratio ($R_{AA}^R/R_{AA}^{R=small}$) as a function of jet radius and jet- p_T , where the observations are well described by the JETSCAPE framework which is based on the hydrodynamic multi-stage evolution of the parton shower. The calculations are then replicated for different low-virtuality based evolution models like the MARTINI and the AdS/CFT, which is followed by a rigorous comparison between the predictions from the former model combinations to the measurements at the CMS experiment.

I. INTRODUCTION

The extremely hot and dense conditions created at the starting of big bang which we now understand as the soup of de-confined state of the partons, the Quark-Gluon Plasma. The QGP is of such great interest that, to study the properties of this state of matter, scientists have spent decades in building up the equipment which could recreate this extremely dense soupy state. The Relativistic Heavy-Ion Collider (RHIC) and the Large Hadron Collider (LHC) conduct Heavy-ion collisions where the QGP is created for very short instants of time, the parton shower propagation and modification is greatly influenced by the quark-gluon plasma. The high- p_T jets produced in these heavy ion collisions undergo strong yield suppression and medium modification which are together referred to as jet quenching phenomena. Therefore, we study the jet modification in nucleus-nucleus collisions relative to proton-proton collisions to probe the properties of the QGP via constraints from model-to-data comparison. [1–7] The jet Nuclear Modification Factor (R_{AA}) has been one of the most important and the prime observable to study the properties of the Quark-gluon Plasma. The measurement of Nuclear Modification Factor for jets as well as charged particles has revealed many important characteristics of the Quark-gluon plasma. It provides a strong confirmation of the interaction of partons with the deconfined plasma, the respective medium modifications and the eventual hydrodynamization with the medium [8]. Since there are many conclusive studies based on jet- R_{AA} [9–13], our effort here is to push the limits of what we hope to learn about the QGP from this observable with the available experimental data.

Along with these measurements, we can reconstruct in-

clusive jet spectra for p-p and Pb-Pb by varying distance parameters R in the anti- k_T algorithm, which is realized in the FASTJET software package [14]. The inclusive jet spectrum is of significant interest because the sensitivity of hadronization effects is far less compared to the observables involving individual final-state hadrons. Here, the area of the reconstructed jet cone is defined by R . Thus, by varying R , the reconstructed jet will include different proportions of energy from the medium response and the quenched jet. We have also observed new sensitivity to QGP properties and underlying jet quenching mechanism in a study for jet yield suppression versus R [15]. Specifically, different dependences of the jet suppression on R , are predicted by generators and theoretical models based on anti-de Sitter/conformal field theory correspondence [16] and perturbative QCD [17].

We take off by calculating the Jet (R_{AA}) for the Pb-Pb collisions in SECTION II and compare with the experimental data from the ATLAS as well as the CMS detector for a robust test of our configuration and the overall JETSCAPE Framework (version 3.5.1) [18]. Our calculations include the (2+1)D MUSIC [19] model for hydrodynamics which is ideal for studying many aspects of heavy ion collisions. Most notably, our calculations cover the high- p_T range of jets that is up to 1 TeV, which enables us to probe the medium at much shorter distance scales.

We now exploit the advantages that the JETSCAPE framework offers in SECTION II A, that is the coupling of several different energy loss modules such as MARTINI and AdS/CFT with the MATTER module to explore the quenching effects in a multi-stage manner which gives us an insight into the interaction and energy loss mechanism in the medium with respect to the virtuality of the partonic jet. Comparing the experimental data with the trends from these different models which handle the low virtuality phase allows us to develop a lucid understanding of the physics governing the above models.

* Corresponding author: prabhakar.palni@unigoa.ac.in

In SECTION II B, we proceed with concrete results from the above combinations of several successful models towards the jet radius dependence studies. An important measurement done by the CMS collaboration [20] recently, was the jet- R_{AA} for Pb-Pb collisions at the LHC and recording the data for jet cone area covering the radii from 0.2 up to 1. This analysis gives us an intricate understanding of the behaviour and interaction strength of the high- p_T inclusive collimated jets in proximity to the jet axis, for $R=0.2$ and the energy distribution around the cone for values of radii up to 1. The current JETSCAPE framework is based on calculations of perturbative quantum chromodynamics and evolution in a dense medium, thus allowing us to go up to a radius of order 1. We also plot and report the Double Ratio for jet- p_T dependence and jet radius dependence to provide a vivid picture of the energy transactions with the Quark-gluon plasma as the jet cone size increases and also discuss the trends that the JETSCAPE framework predicts.

We conclude this work in SECTION III, with a concise account of the current JETSCAPE model's potential to explain the jet- R_{AA} for larger area jet cones. We also shed light on the ability of the distinct combination of modules to describe the jet- R_{AA} .

A. SIMULATION WITH MULTI-STAGE ENERGY LOSS APPROACH IN JETSCAPE

The JETSCAPE framework provides an ideal environment for carrying out multi-stage energy loss. The hard scattering is generated by PYTHIA 8 [21] with initial state radiation (ISR) and multiparton interaction (MPI) turned on, and final state radiation (FSR) turned off. For the event wise simulations, the TRENTo model [22] sets up the initial conditions and the viscous hydrodynamic evolution is described by the (2+1)D MUSIC [19] model followed by Cooper-Frye prescription [23, 24] which converts the fluid cells to hadrons on an isothermal hypersurface at $T_{SW}=151$ MeV. The jet energy loss induced by scattering is calculated in succession of two stages: MATTER [25, 26] takes care of the highly virtual phase (the first stage) while the low virtuality phase (the second stage), is handled concurrently by the LBT model [27–29]. We have also employed the MARTINI [30–32] and the AdS/CFT model [33] in combination with the MATTER model to explore the low virtuality phase. the virtuality of the parton is defined as Q . The parton undergoes energy loss in two stages, when the virtuality of the parton, $Q^2 > Q_{SW}^2$, where Q_{SW} is the switching virtuality, the MATTER model handles the energy loss and the parton is transferred to the LBT model once $Q^2 \leq Q_{SW}^2$. In our calculations, the jet medium interaction includes inelastic medium-induced gluon radiation and medium recoil. An extensive account on the comparison of the model to the existing jet- R_{AA} is already done [34], showing that the contribution of medium recoil is pretty significant in the modification of jet- R_{AA}

for a complete set of centrality classes ranging from the most central collisions to the peripheral collisions. This version of the JETSCAPE framework [18] encompasses the modifications of a hard thermal-loop (HTL) \hat{q} [35] for fixed coupling, running coupling, and with a virtuality dependent factor that modulates the effective value of \hat{q} . It also accounts for the reduced medium-induced emission in the high virtuality phase, due to coherence effects. The calculations based on the hard-thermal-loop (HTL) considering weak- coupling approximation and the limits of high temperature yield a \hat{q} given as [28],

$$\hat{q}_{HTL} = C_a \frac{42\zeta(3)}{\pi} \alpha_s^2 T^3 \ln \left[\frac{2ET}{6\pi T^2 \alpha_s^{\text{fix}}} \right]. \quad (1)$$

where C_a is the representation specific Casimir, E is the energy of the hard parton and T is the local temperature of the medium. The Coherence effects which reduce the interaction strength of the parton with the medium is also taken into consideration as the virtuality dependent modulation factor $f(Q^2)$ which regulates the effective value of \hat{q} in the high virtuality MATTER event generator. The parameterization of the virtuality-dependent modulation factor is given as [34]

$$\hat{q} \cdot f \equiv \hat{q}_{HTL}^{\text{run}} f(Q^2) \quad (2)$$

$$f(Q^2) = \begin{cases} \frac{1+10 \ln^2(Q_{sw}^2)+100 \ln^4(Q_{sw}^2)}{1+10 \ln^2(Q^2)+100 \ln^4(Q^2)} & Q^2 > Q_{sw}^2 \\ 1 & Q^2 \leq Q_{sw}^2 \end{cases}, \quad (3)$$

here Q^2 is the running virtuality of the hard parton. Finally, the partons undergo colorless hadronization according to the default Lund string fragmentation from PYTHIA 8 [21, 36]. The major contributions in our final jets are from hard jet shower part and the effect from the soft medium response, the latter is calculated via the Cooper-Frye formula. We reconstruct our jets for several radius selections using the anti- k_T algorithm which is realised in the FASTJET Software Package [14] and compare with experimental data. The Underlying Events (UE) are removed by implementing a minimum track requirement of $p_T^{\text{track, min}} > 4$ GeV. All the parameters involved in the tuning of the constituent modules follow the standard set of tunes released by the JETSCAPE Collaboration in an elaborate recent study [34].

II. RESULTS AND ANALYSIS

This work covers the collision energy: $\sqrt{s_{NN}} = 5.02$ TeV for two centrality classes i.e.the most central(0-10%) collisions and shows a comparison with selected experimental data available from the ATLAS and the CMS Collaborations. The energy loss depicted in our results is achieved by the coupling of MATTER with the LBT module and the secondary module (which handles the low virtuality phase) remains the same throughout our results until and unless specified. Fig. 1 shows the $p + p$ simulation results for inclusive jet spectra for

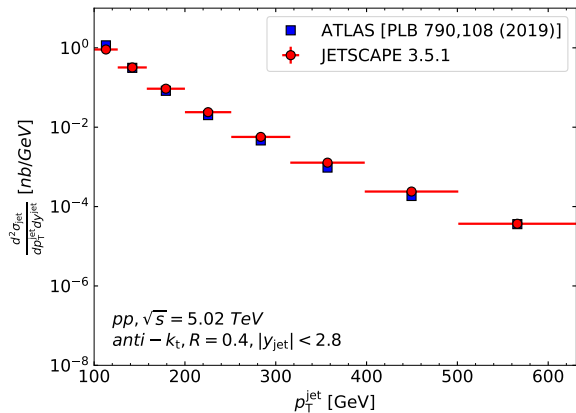


FIG. 1. (Color online) Differential cross section of inclusive jets for p+p collisions with cone size $R=0.4$, with a minimum track requirement of $p_T^{\text{track}} > 4$ GeV.

p+p at $\sqrt{s} = 5.02\text{TeV}$ for $|y_{jet}| < 2.8$ which follow the JETSCAPE PP 19 tune [37] are then compared to the experimental data from the ATLAS [12, 13], the ratio of inclusive jet cross-section to the ATLAS data is plotted in fig. 2, which clearly shows that the results are in acceptable range ($\leq 20\%$). We report the 0-10% central Pb-Pb jet spectra for $R=0.4$ in fig. 3. We also plot the ratio of differential cross section for inclusive jets compared to the data from ATLAS [13] shown in fig. 4. Here, R_{AA} is defined as

$$R_{AA} = \frac{1}{N_{\text{event}}} \frac{d^2 N_{\text{jet}}}{d\eta_{\text{jet}} dp_T^{\text{jet}}} \Big|_{AA}, \quad (4)$$

$$\frac{d^2 \sigma_{\text{jet}}}{d\eta_{\text{jet}} dp_T^{\text{jet}}} \Big|_{pp}$$

The inclusive jet- R_{AA} is now calculated as the ratio of the Pb-Pb and p-p spectra plotted above, which is shown in fig. 5 in comparison to the ATLAS data. The JETSCAPE results agree with the data quite nicely, although we see a 5% enhancement in the low p_T region which is followed by a suppression as we ascend in the range.

A. Exploring the MARTINI and AdS/CFT models

Both the MARTINI [30] and the AdS/CFT [33] models are designed to handle the low virtuality phase and carry forward the energy loss once the parton is transferred from the MATTER. We now replace the successful LBT model with the MARTINI model, to carry out the simulations for the same settings [34] and compare the jet- R_{AA} with the experimental data from the ATLAS Collaboration [13]. Similarly the calculations are done by replacing the LBT by AdS/CFT and compared with the recorded data.

We now present the intensive comparison between the low virtuality parton evolution models, where the in-

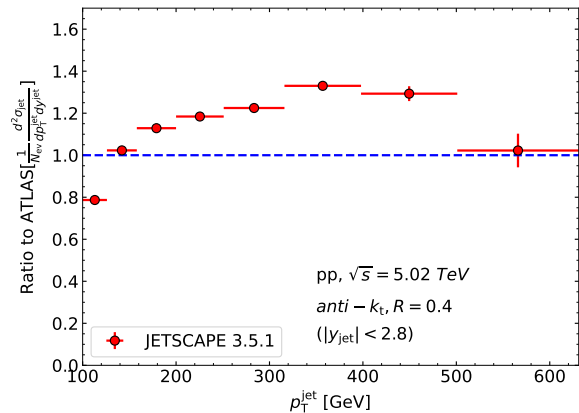


FIG. 2. (Color online) Differential cross-section of inclusive jets for p+p collisions with cone size $R=0.4$, with a minimum track requirement of $p_T^{\text{track}} > 4$ GeV.

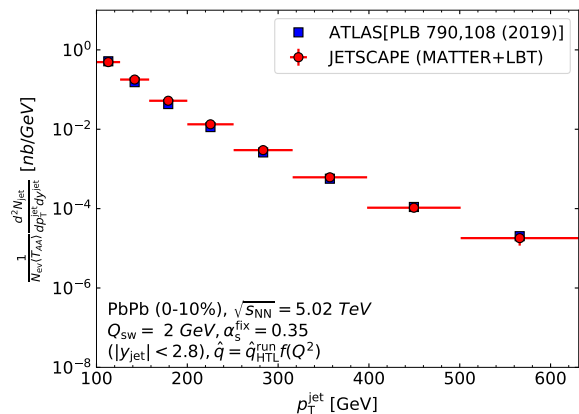


FIG. 3. (Color online) Differential cross-section of inclusive jets in Pb+Pb collisions at $\sqrt{s_{NN}} = 5.02\text{TeV}$ with cone size $R=0.4$, with a minimum track requirement of $p_T^{\text{track}} > 4$ GeV.

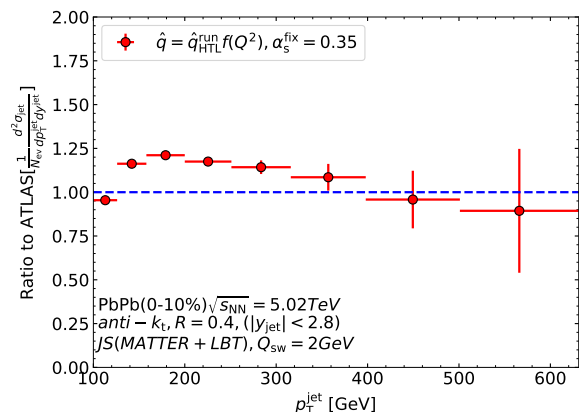


FIG. 4. (Color online) Ratio of differential cross section for inclusive jets with cone size $R = 0.4$ in Pb+Pb collisions at $\sqrt{s_{NN}} = 5.02\text{TeV}$. The ratio is taken with respect to the ATLAS data [cite].

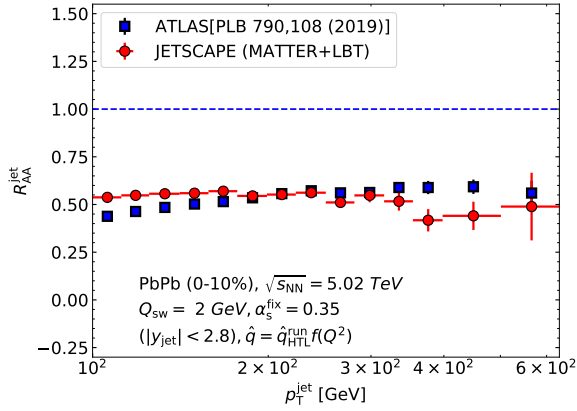


FIG. 5. (Color online) the jet- R_{AA} as a function of jet- p_T for inclusive jets in the most central(0-10%) Pb+Pb collisions at $\sqrt{s_{NN}} = 5.02$ TeV for the jet cone radius $R=0.4$ with $|y_{jet}| < 2.8$ and a minimum track requirement of $p_T^{\text{track}} > 4$ GeV.

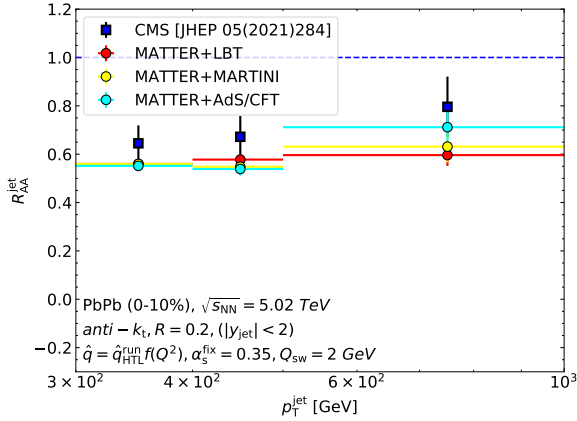


FIG. 6. (Color online) the jet- R_{AA} as a function of jet- p_T for inclusive jets in the most central(0-10%) Pb+Pb collisions at $\sqrt{s_{NN}} = 5.02$ TeV for the jet cone radius $R=0.2$ with $|y_{jet}| < 2$ and a minimum track requirement of $p_T^{\text{track}} > 4$ GeV. The plot shows the comparison between the models by red, yellow and cyan markers for (MATTER+LBT), (MATTER+MARTINI) and (MATTER+AdS/CFT), respectively. The predictions are in comparison with CMS data shown with blue marker.

clusive jet- R_{AA} is calculated for three models, MATTER coupled with LBT (which is our default), MATTER coupled with MARTINI and MATTER coupled with AdS/CFT, the simulations are altogether staged in contrast with the experimental data.

The above calculations for different models are extended and fig. 6 shows the jet- R_{AA} for $|y_{jet}| < 2$ and jet cone radius $R=0.2$, in comparison with the experimental data from the CMS Collaboration [20]. Similarly, the jet- R_{AA} is plotted for $R=0.4$, $R=0.6$, $R=0.8$ and $R=1.0$ in the fig. 7, fig. 8, fig. 9 and fig. 10 respectively. The

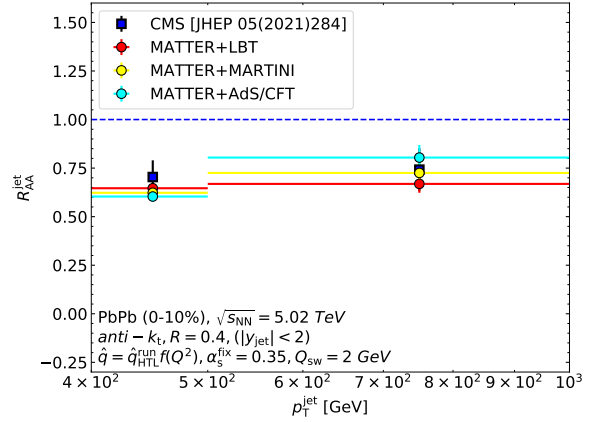


FIG. 7. (Color online) the jet- R_{AA} as a function of jet- p_T for inclusive jets in the most central(0-10%) Pb+Pb collisions at $\sqrt{s_{NN}} = 5.02$ TeV for the jet cone radius $R=0.4$ with $|y_{jet}| < 2$ and a minimum track requirement of $p_T^{\text{track}} > 4$ GeV. The plot shows the comparison between the models by red, yellow and cyan markers for (MATTER+LBT), (MATTER+MARTINI) and (MATTER+AdS/CFT), respectively. The predictions are in comparison with CMS data shown with blue marker.

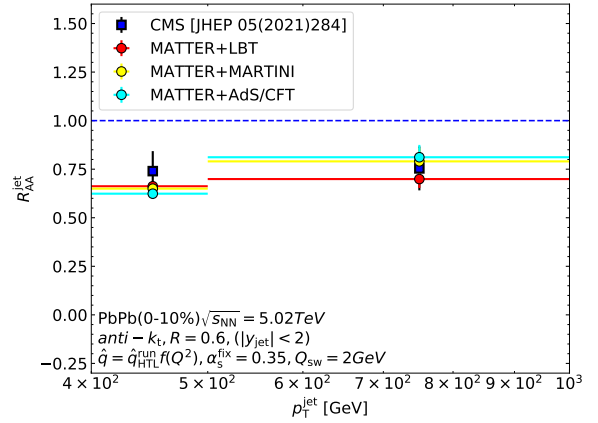


FIG. 8. (Color online) the jet- R_{AA} as a function of jet- p_T for inclusive jets in the most central(0-10%) Pb+Pb collisions at $\sqrt{s_{NN}} = 5.02$ TeV for the jet cone radius $R=0.6$ with $|y_{jet}| < 2$ and a minimum track requirement of $p_T^{\text{track}} > 4$ GeV. The plot shows the comparison between the models by red, yellow and cyan markers for (MATTER+LBT), (MATTER+MARTINI) and (MATTER+AdS/CFT), respectively. The predictions are in comparison with CMS data shown with blue marker.

predictions made by the JETSCAPE are consistent even as we move to larger area jet cones. The radiative energy loss in AdS/CFT is more dominant than the elastic jet energy loss compared to LBT and MARTINI. Since, the effect of the recoil partons in LBT on the total energy loss is not very significant. It is very articulate that there is an appreciable reduction in net elastic and radiative jet

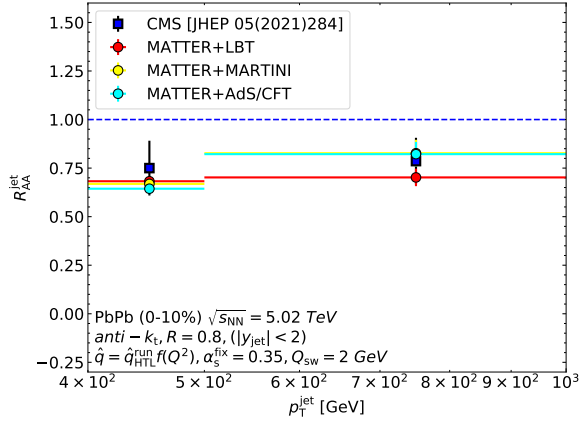


FIG. 9. (Color online) the jet- R_{AA} as a function of jet- p_T for inclusive jets in the most central(0-10%) Pb+Pb collisions at $\sqrt{s_{NN}} = 5.02$ TeV for the jet cone radius $R=0.8$ with $|y_{jet}| < 2$ and a minimum track requirement of $p_T^{\text{track}} > 4$ GeV. The plot shows the comparison between the models by red, yellow and cyan markers for (MATTER+LBT), (MATTER+MARTINI) and (MATTER+AdS/CFT), respectively. The predictions are in comparison with CMS data shown with blue marker.

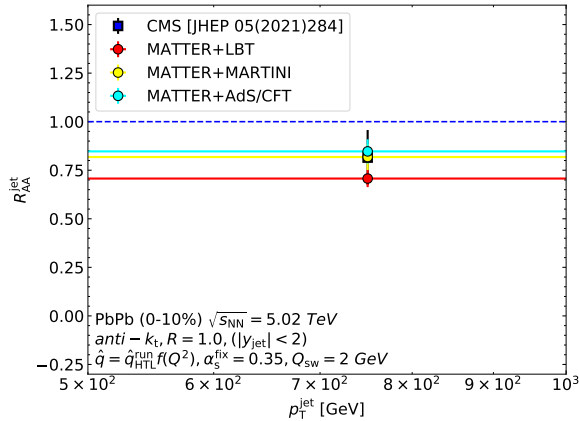


FIG. 10. (Color online) the jet- R_{AA} as a function of jet- p_T for inclusive jets in the most central(0-10%) Pb+Pb collisions at $\sqrt{s_{NN}} = 5.02$ TeV for the jet cone radius $R=1.0$ with $|y_{jet}| < 2$ and a minimum track requirement of $p_T^{\text{track}} > 4$ GeV. The plot shows the comparison between the models by red, yellow and cyan markers for (MATTER+LBT), (MATTER+MARTINI) and (MATTER+AdS/CFT), respectively. The predictions are in comparison with CMS data shown with blue marker.

energy loss when the jet cone includes the recoil partons.

With the above comparisons to both ATLAS and CMS experimental data, the simulation results from the JETSCAPE stand sturdy for credible studies using the current model, which is carried out in the next section.

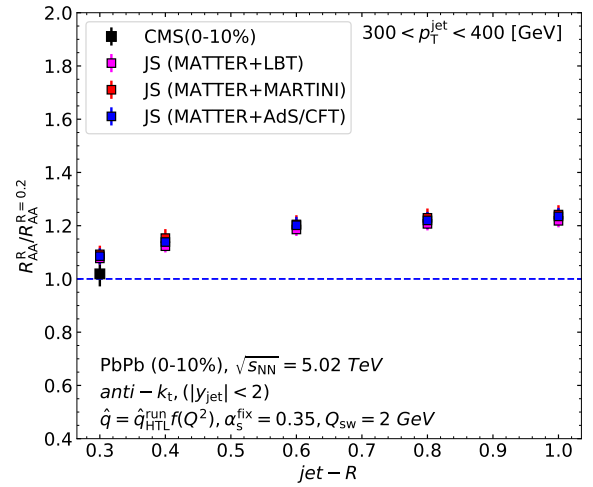


FIG. 11. (Color online) ($300 \text{ GeV} \leq p_{T,jet} \leq 400 \text{ GeV}$) the double ratio ($R_{AA}^R / R_{AA}^{R=0.2}$) as a function of jet radius for inclusive jets in the most central(0-10%) Pb+Pb collisions at $\sqrt{s_{NN}} = 5.02$ TeV for different jet radii with $|y_{jet}| < 2$ and a minimum track requirement of $p_T^{\text{track}} > 4$ GeV. The plot shows the comparison between the models by magenta, red and blue markers for (MATTER+LBT), (MATTER+MARTINI) and (MATTER+AdS/CFT), respectively. The predictions are in comparison with CMS data shown with black marker.

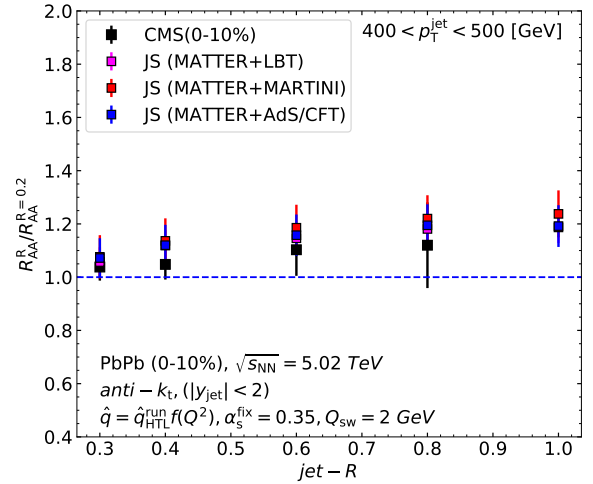


FIG. 12. (Color online) ($400 \text{ GeV} \leq p_{T,jet} \leq 500 \text{ GeV}$) the double ratio ($R_{AA}^R / R_{AA}^{R=0.2}$) as a function of jet radius for inclusive jets in the most central(0-10%) Pb+Pb collisions at $\sqrt{s_{NN}} = 5.02$ TeV for different jet radii with $|y_{jet}| < 2$ and a minimum track requirement of $p_T^{\text{track}} > 4$ GeV. The plot shows the comparison between the models by magenta, red and blue markers for (MATTER+LBT), (MATTER+MARTINI) and (MATTER+AdS/CFT), respectively. The predictions are in comparison with CMS data shown with black marker.

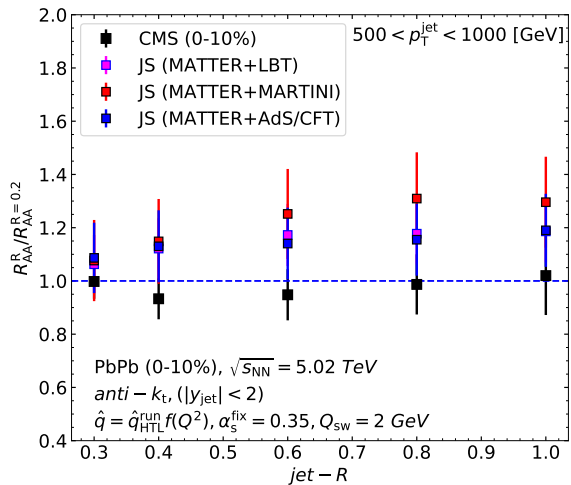


FIG. 13. (Color online) ($500 \text{ GeV} \leq p_{T,jet} \leq 1 \text{ TeV}$) the double ratio ($R_{AA}^R/R_{AA}^{R=0.2}$) as a function of jet radius for inclusive jets in the most central (0-10%) Pb+Pb collisions at $\sqrt{s_{NN}} = 5.02 \text{ TeV}$ for different jet radii with $|y_{jet}| < 2$ and a minimum track requirement of $p_T^{\text{track}} > 4 \text{ GeV}$. The plot shows the comparison between the models by magenta, red and blue markers for (MATTER+LBT), (MATTER+MARTINI) and (MATTER+AdS/CFT), respectively. The predictions are in comparison with CMS data shown with black marker.

B. jet- p_T and jet radius dependence of the R_{AA}

In this section we emphasise on the the significant contribution from the hydrodynamic medium response already highlighted in previous studies [8, 38], which is observed in the jet- R_{AA} as a function of jet radius. Through radius dependent studies, we hope to develop a clear picture of the parts played by radiation and collisions in energy loss.

In a recent study by the CMS Collaboration [20], where they have compared predictions from quenched jet event generators and theoretical models used to replicate relativistic heavy ion collisions to the experimental data for the jet- R_{AA} . They arrive at the conclusion that although most state of the art models have progressed but significant uncertainty remains for the large area jet data. The large jet radius R also implies that the jet retains a significant proportion of the extensively distributed momentum and energy deposited in the plasma. Since, the JETSCAPE framework has pioneered the realisation of multi-stage approach for modular based energy loss, the motivation here is to challenge the JETSCAPE model that has so far met our expectations in describing the variety of data observed and to explore the boundaries of the current model.

This quest is executed by calculating the double ratio ($R_{AA}^R/R_{AA}^{R=0.2}$) and plotting as a function of jet radius which are in comparison with the data for the most central (0-10%) Pb-Pb collisions over a range of jet- p_T

from 200 GeV up to 1 TeV. The plots are further sub-categorized by three jet- p_T bins.

For $300 \text{ GeV} \leq p_{T,jet} \leq 400 \text{ GeV}$, fig x shows the predictions by the different combination of energy loss models and we see a consistent trend for all three models i.e. (MATTER+LBT), (MATTER+MARTINI) and (MATTER+AdS/CFT), the results are within the statistical limits.

For $400 \text{ GeV} \leq p_{T,jet} \leq 500 \text{ GeV}$, we observe in fig. y, that (MATTER+LBT) is in fine agreement with the data while both (MATTER+MARTINI) and (MATTER+AdS/CFT), tend to slightly over-predict the jet- $R_{AA}(\leq 10\%)$.

In the extreme region i.e. for $500 \text{ GeV} \leq p_{T,jet} \leq 1 \text{ TeV}$, all the models significantly over-predict the jet- R_{AA} , with the best description provided by the (MATTER+LBT) model ($\leq 10\%$). All the models show saturation around jet radius $R=0.8$ and $R=1.0$, which fits well for a realistic approach. Altogether, the JETSCAPE framework nicely describes the full evolution of the parton shower by adopting a virtuality based multi-stage approach for energy loss. We observe that as the jet is scattered in the medium, the final state partons of the medium interacting with the jet are also considered as a constituent of the jet. As more and more gluons fall into the larger jet cone and prohibit from contributing to the jet energy loss. Therefore, energy lost by the jets is partially gained as the area of jet cone increases.

III. CONCLUSION

In this paper, we present the first comparisons of the jet- R_{AA} predictions from the JETSCAPE framework using the (2+1)D MUSIC model for viscous hydrodynamic evolution to the ATLAS data for Pb+Pb collisions at $\sqrt{s_{NN}} = 5.02 \text{ TeV}$ in high jet transverse momentum interval $100 \text{ GeV} \leq p_{T,jet} \leq 1 \text{ TeV}$ for anti- k_T jets of radius $R=0.4$. The above results put us in a strong stance to conclude that the MUSIC model is adequate and also successful in speculating the experimental observations even at higher jet- p_T for the most central collisions as well as mid-central collisions.

This work also elucidates the predictions made by low virtuality based evolution models like MARTINI and AdS/CFT in a hydrodynamic medium generated by the MUSIC. We observe an overall similar trend anticipations as compared to the unfolding in other hydrodynamic models like (2+1)D VISHNU [39].

We advance the current JETSCAPE calculations and compare with the data of wider jet cones ranging from $R=0.2$ to $R=1.0$ recorded at the CMS detector for Pb+Pb collisions at $\sqrt{s_{NN}} = 5.02 \text{ TeV}$ in high jet transverse momentum interval $200 \text{ GeV} \leq p_{T,jet} \leq 1 \text{ TeV}$ for anti- k_T jets of radii $R=0.2, 0.4, 0.6, 0.8$ and 1.0 . Although the JETSCAPE framework is still under improvisation to define the jet medium interactions at wide angles, this

work highlights the current standing of the model to describe the energy loss and medium response phenomenon for broad area jet cones and the JETSCAPE predictions are well within the statistical errors.

IV. ACKNOWLEDGEMENTS

The authors would like to acknowledge Yasuki Tachibana and Chun Shen for their useful discussion and feedback. The authors would also like to thank Goa University Param computing facility and seed money grant support.

-
- [1] J. D. Bjorken, Energy Loss of Energetic Partons in Quark - Gluon Plasma: Possible Extinction of High $p(t)$ Jets in Hadron - Hadron Collisions, (1982).
- [2] D. A. Appel, Jets as a Probe of Quark - Gluon Plasmas, *Phys. Rev. D* **33**, 717 (1986).
- [3] R. Baier, Y. L. Dokshitzer, A. H. Mueller, S. Peigne, and D. Schiff, Radiative energy loss of high-energy quarks and gluons in a finite volume quark - gluon plasma, *Nucl. Phys. B* **483**, 291 (1997), [arXiv:hep-ph/9607355](#).
- [4] R. Baier, Y. L. Dokshitzer, A. H. Mueller, S. Peigne, and D. Schiff, Radiative energy loss and $p(T)$ broadening of high-energy partons in nuclei, *Nucl. Phys. B* **484**, 265 (1997), [arXiv:hep-ph/9608322](#).
- [5] B. G. Zakharov, Fully quantum treatment of the Landau-Pomeranchuk-Migdal effect in QED and QCD, *JETP Lett.* **63**, 952 (1996), [arXiv:hep-ph/9607440](#).
- [6] M. Gyulassy, P. Levai, and I. Vitev, Jet quenching in thin quark gluon plasmas. 1. Formalism, *Nucl. Phys. B* **571**, 197 (2000), [arXiv:hep-ph/9907461](#).
- [7] M. Gyulassy, P. Levai, and I. Vitev, NonAbelian energy loss at finite opacity, *Phys. Rev. Lett.* **85**, 5535 (2000), [arXiv:nucl-th/0005032](#).
- [8] N.-B. Chang, Y. Tachibana, and G.-Y. Qin, Nuclear modification of jet shape for inclusive jets and γ -jets at the LHC energies, *Physics Letters B* **801**, 135181 (2020).
- [9] ATLAS Collaboration, Measurement of substructure-dependent jet suppression in pb+pb collisions at 5.02 tev with the atlas detector (2022).
- [10] A. M. Sirunyan *et al.* (CMS), In-medium modification of dijets in PbPb collisions at $\sqrt{s_{NN}} = 5.02$ TeV, *JHEP* **05**, 116, [arXiv:2101.04720 \[hep-ex\]](#).
- [11] G. Aad *et al.* (ATLAS), Measurement of the jet radius and transverse momentum dependence of inclusive jet suppression in lead-lead collisions at $\sqrt{s_{NN}} = 2.76$ TeV with the ATLAS detector, *Phys. Lett. B* **719**, 220 (2013), [arXiv:1208.1967 \[hep-ex\]](#).
- [12] M. Aaboud *et al.* (ATLAS), Measurement of the nuclear modification factor for inclusive jets in Pb+Pb collisions at $\sqrt{s_{NN}} = 5.02$ TeV with the ATLAS detector, *Phys. Lett. B* **790**, 108 (2019), [arXiv:1805.05635 \[nucl-ex\]](#).
- [13] Measurement of substructure-dependent jet suppression in Pb+Pb collisions at 5.02 TeV with the ATLAS detector, (2022), [arXiv:2211.11470 \[nucl-ex\]](#).
- [14] M. Cacciari, G. P. Salam, and G. Soyez, FastJet User Manual, *Eur. Phys. J. C* **72**, 1896 (2012), [arXiv:1111.6097 \[hep-ph\]](#).
- [15] Y.-T. Chien and I. Vitev, Towards the understanding of jet shapes and cross sections in heavy ion collisions using soft-collinear effective theory, *Journal of High Energy Physics* **2016**, 10.1007/jhep05(2016)023 (2016).
- [16] Z. Hulcher, D. Pablos, and K. Rajagopal, Resolution effects in the hybrid strong/weak coupling model, *Journal of High Energy Physics* **2018**, 10.1007/jhep03(2018)010 (2018).
- [17] N. Armesto, L. Cunqueiro, and C. A. Salgado, Q-PYTHIA: a medium-modified implementation of final state radiation, *The European Physical Journal C* **63**, 10.1140/epjc/s10052-009-1133-9 (2009).
- [18] J. H. Putschke *et al.*, The JETSCAPE framework, (2019), [arXiv:1903.07706 \[nucl-th\]](#).
- [19] B. Schenke, S. Jeon, and C. Gale, (3+1)d hydrodynamic simulation of relativistic heavy-ion collisions, *Physical Review C* **82**, 10.1103/physrevc.82.014903 (2010).
- [20] A. M. Sirunyan *et al.* (CMS), First measurement of large area jet transverse momentum spectra in heavy-ion collisions, *JHEP* **05**, 284, [arXiv:2102.13080 \[hep-ex\]](#).
- [21] T. Sjöstrand, The PYTHIA Event Generator: Past, Present and Future, *Comput. Phys. Commun.* **246**, 106910 (2020), [arXiv:1907.09874 \[hep-ph\]](#).
- [22] J. S. Moreland, J. E. Bernhard, and S. A. Bass, Alternative ansatz to wounded nucleon and binary collision scaling in high-energy nuclear collisions, *Phys. Rev. C* **92**, 011901 (2015), [arXiv:1412.4708 \[nucl-th\]](#).
- [23] V. Vovchenko, Cooper-frye sampling with short-range repulsion, *Physical Review C* **106**, 10.1103/physrevc.106.064906 (2022).
- [24] M. McNelis and U. Heinz, Modified equilibrium distributions for cooper-frye particlization, *Physical Review C* **103**, 10.1103/physrevc.103.064903 (2021).
- [25] S. Cao and A. Majumder, Nuclear modification of leading hadrons and jets within a virtuality ordered parton shower, *Phys. Rev. C* **101**, 024903 (2020), [arXiv:1712.10055 \[nucl-th\]](#).
- [26] A. Majumder, Incorporating Space-Time Within Medium-Modified Jet Event Generators, *Phys. Rev. C* **88**, 014909 (2013), [arXiv:1301.5323 \[nucl-th\]](#).
- [27] F.-L. Liu, W.-J. Xing, X.-Y. Wu, G.-Y. Qin, S. Cao, and X.-N. Wang, QLBT: a linear Boltzmann transport model for heavy quarks in a quark-gluon plasma of quasi-particles, *Eur. Phys. J. C* **82**, 350 (2022), [arXiv:2107.11713 \[hep-ph\]](#).
- [28] Y. He, T. Luo, X.-N. Wang, and Y. Zhu, Linear Boltzmann Transport for Jet Propagation in the Quark-Gluon Plasma: Elastic Processes and Medium Recoil, *Phys. Rev. C* **91**, 054908 (2015), [Erratum: *Phys. Rev. C* **97**, 019902 (2018)], [arXiv:1503.03313 \[nucl-th\]](#).
- [29] S. Cao, T. Luo, G.-Y. Qin, and X.-N. Wang, Linearized Boltzmann transport model for jet propagation in the quark-gluon plasma: Heavy quark evolution, *Phys. Rev. C* **94**, 014909 (2016), [arXiv:1605.06447 \[nucl-th\]](#).
- [30] B. Schenke, C. Gale, and S. Jeon, MARTINI: An Event generator for relativistic heavy-ion collisions, *Phys. Rev. C* **80**, 054913 (2009), [arXiv:0909.2037 \[hep-ph\]](#).

- [31] S. Shi, R. Modarresi Yazdi, C. Gale, and S. Jeon, Comparing the MARTINI and CUJET models for jet quenching: I. medium modification of jets and jet substructure, (2022), [arXiv:2212.05944 \[hep-ph\]](#).
- [32] R. M. Yazdi, S. Shi, C. Gale, and S. Jeon, Leading order, next-to-leading order, and nonperturbative parton collision kernels: Effects in static and evolving media, *Phys. Rev. C* **106**, 064902 (2022), [arXiv:2206.05855 \[hep-ph\]](#).
- [33] J. L. Albacete, Y. V. Kovchegov, and A. Taliotis, Modeling heavy ion collisions in AdS/CFT, *Journal of High Energy Physics* **2008**, 100 (2008).
- [34] A. Kumar *et al.* (JETSCAPE), Inclusive Jet and Hadron Suppression in a Multi-Stage Approach, (2022), [arXiv:2204.01163 \[hep-ph\]](#).
- [35] Y. Hidaka and R. D. Pisarski, Hard thermal loops, to quadratic order, in the background of a spatial 't hooft loop, *Physical Review D* **80**, [10.1103/physrevd.80.036004](#) (2009).
- [36] N. Armesto, L. Cunqueiro, and C. A. Salgado, Q-PYTHIA: A Medium-modified implementation of final state radiation, *Eur. Phys. J. C* **63**, 679 (2009), [arXiv:0907.1014 \[hep-ph\]](#).
- [37] A. Kumar *et al.* (JETSCAPE), JETSCAPE framework: $p + p$ results, *Phys. Rev. C* **102**, 054906 (2020), [arXiv:1910.05481 \[nucl-th\]](#).
- [38] D. Pablos, Jet suppression from a small to intermediate to large radius, *Physical Review Letters* **124**, [10.1103/physrevlett.124.052301](#) (2020).
- [39] C. Shen, Z. Qiu, H. Song, J. Bernhard, S. Bass, and U. Heinz, The iEBE-VISHNU code package for relativistic heavy-ion collisions, *Comput. Phys. Commun.* **199**, 61 (2016), [arXiv:1409.8164 \[nucl-th\]](#).